JOURNAL OF MOLECULAR SPECTROSCOPY 45, 82–98 (1973)

Absorption Spectrum of BS_2 at 4°K

J. M. BROM, JR. AND W. WELTNER, JR.

Department of Chemistry, University of Florida, Gainesville, Florida 32601

BS_2, trapped in neon matrices at 4°K, exhibits extensive progressions in the $A^2\Pi_u \leftarrow X^2\Pi_g$ and $B^2\Sigma_u^+ \leftarrow X^2\Pi_g$ systems. From these transitions, those observed in the infrared, and a reinterpretation of gas-phase data, the following molecular constants (in solid neon) are obtained for linear symmetric $^{11}BS_2$ (in cm^{-1}):

$B^2\Sigma_u^+$	$T_0 = 24{,}072$	$\nu_1 = 516$
$A^2\Pi_u$	$T_0 = 13{,}766$	$\nu_1 = 506$
	$A_0 = -263$	$\nu_2 = 311$
		$\nu_3 = 1535$
$X^2\Pi_g$	$A_0 = -440$	$\nu_1 = 510$
		$\nu_2 = \sim 120$
		$\nu_3 = 1015$

Vibronic coupling (Renner–Teller effect), although present in the $A^2\Pi_u$ state, is small, as are also any Fermi resonance effects.

INTRODUCTION

Johns (*1*) has made a detailed spectroscopic investigation of the BO_2 molecule in the gas phase. From a rotational analysis of the two electronic transitions, $A^2\Pi_u \leftarrow X^2\Pi_g$ and $B^2\Sigma_u^+ \leftarrow X^2\Pi_g$, observed in absorption, he has shown that the molecule is linear and symmetric in all the observed states. Both Π states exhibit vibronic coupling involving the bending frequency ν_2 (Renner–Teller effect), in addition to spin–orbit interaction. As has generally been found to be true of symmetric triatomics with 15 valence electrons (*2*) the vibronic interaction in the excited $^2\Pi$ state is much smaller than in the ground state.

BS_2 is expected to be similar but with larger spin–orbit coupling constants in the Π states. However, only sketchy reports of spectroscopic investigations of boron sulfide molecules are available in the literature (*3–5*). All the previous studies involved observations of the complex vapor over some condensed phase at high temperatures and were therefore difficult to analyze.

A remarkably detailed absorption spectrum of the BS_2 molecule, containing many analyzable progressions in the region of 7200 to 4000 Å, is reported here. Along with the IR spectrum of the ground state molecule, these data confirm the expected similarity to BO_2 and yield extensive information about its vibrational, vibronic, and spin–orbit properties in the various states.

It should also be mentioned that BS_2 has a role in the high temperature chemistry of the boron-sulfur vapor system. Vaporization studies of sulfur rich samples of B_2S_3(s) (*6*) and BS_2(s) (*7*) have shown that the polymers $(BS_2)_n$ are major constituents of the vapor so that the monomer, BS_2, can serve as a starting point in understanding such complex systems.

EXPERIMENTAL

The liquid helium Dewar and furnace arrangement used for the matrix isolation work have been described previously (*8*). BS_2(g) molecules were produced by vaporizing zinc sulfide and boron mixtures in a double Knudsen cell made of tungsten, shown in Fig. 1. The ZnS-B sample was heated in the cooler portion of the cell at temperatures near 900°C. Mass spectrometric studies (*4*) have shown that the vapor species Zn, BS_2, B_2S_2, and B_2S_3 are thus produced in the approximate ratio of 30:1:2:8. Enhancement of the BS_2 partial pressure in the effusing molecular beam was accomplished by passing the saturated vapor through the hotter cell, independently heated to about 1750°C.

The ZnS powder (Matheson, Coleman, and Bell, reagent grade) and isotopically enriched B powder (Union Carbide Nuclear Company, ~95% enrichment of ^{10}B and of ^{11}B) were used without further purification except for outgassing at several hundred degrees prior to an experiment.

Neon matrices were prepared by the simultaneous deposition of the boron sulfides and rare gas upon a CsI window cooled to 4°K. The neon flow rate was maintained at ~0.5 l atm/h, and the gas was precooled with a liquid nitrogen bath immediately before entering the Dewar.

Optical spectra were recorded over the range 3500 Å–12,000 Å. A Jarrell-Ash 0.5 m Ebert scanning spectrophotometer with gratings blazed at 5000 and 10,000 Å, and

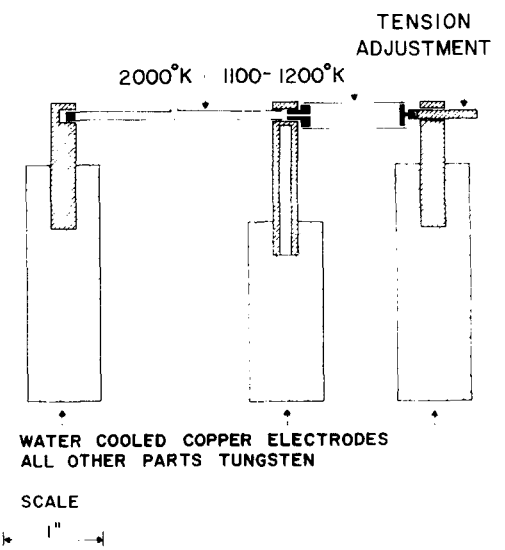

FIG. 1. Tungsten double Knudsen cell.

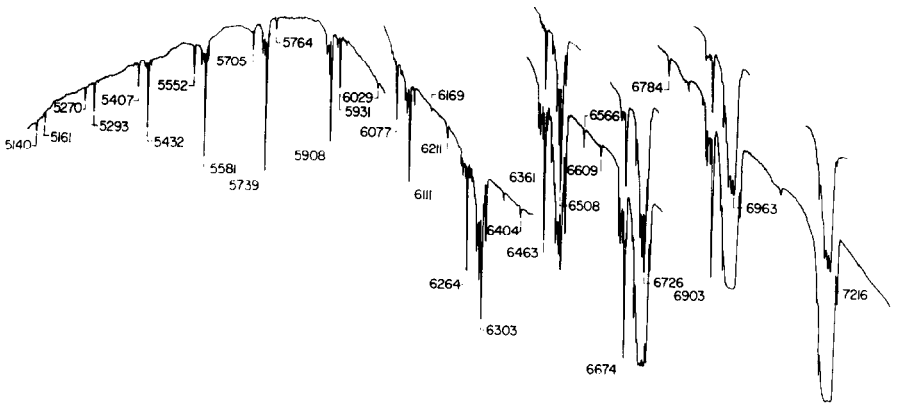

FIG. 2. Absorption spectrum of the A system of $^{11}BS_2$ isolated in Ne at 4°K. Wavelengths are in Å.

equipped with RCA 931A or 7102 photomultiplier tubes, was used in the regions 3500–7500 Å and 7000–12,000 Å, respectively. A tungsten lamp was used as the continuum light source. Relative band positions are generally measureable to ±0.5 Å although absolute positions as determined by Hg arc lines are considered accurate to about ±1 Å. Infrared spectra were recorded from 4000–200 cm^{-1} using a Perkin–Elmer 621 grating spectrophotometer.

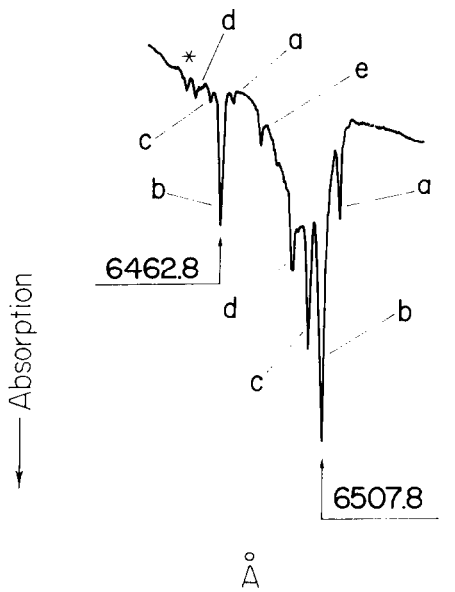

FIG. 3. Expanded scale spectrum of the $^{11}BS_2$ 6507.8 and 6462.8 Å bands showing sub-bands due to multiple trapping sites in Ne at 4°K. The weak band labeled with an asterisk is due to $^{10}BS_2$ in the sample.

TABLE I

ABSORPTION BANDS OF $^{11}BS_2$ A SYSTEM IN NEON AT 4°K

λ, Å[a]	Intensities[b]	λ, Å[a]	Intensities[b]
7216.0	0.93	6111.2	0.10
6962.5	1.00	6076.7	0.04
6903.0	0.16	6029.3	0.00
6784.3	0.01	5931.0	0.03
6725.8	0.91	5907.3	0.09
6674.0	0.21	5763.8	0.01
6609.3	0.01	5739.0	0.12
6565.5	0.01	5704.5	0.01
6507.8	0.80	5580.4	0.09
6462.5	0.15	5551.7	0.02
6404.5	0.01	5432.0	0.05
6361.3	0.01	5407.0	0.01
6302.8	0.36	5292.5	0.02
6263.0	0.08	5269.5	0.01
6211.5	0.01	5161.0	0.00
6168.5	0.00	5140.0	0.00

[a] Band positions are for sub-band *b* due to BS_2 in the predominant trapping site.

[b] Approximate intensities from peak height measurements are given relative to the 6962.5 Å band.

RESULTS

1. Visible Absorption Spectra

The observed visible spectra of BS_2 consist of two systems designated A and B in analogy with BO_2 (*1*): system A beginning at 7200 Å with an extensive series of progressions developed out to 5100 Å; system B at 4116 Å and extending to 3952 Å.

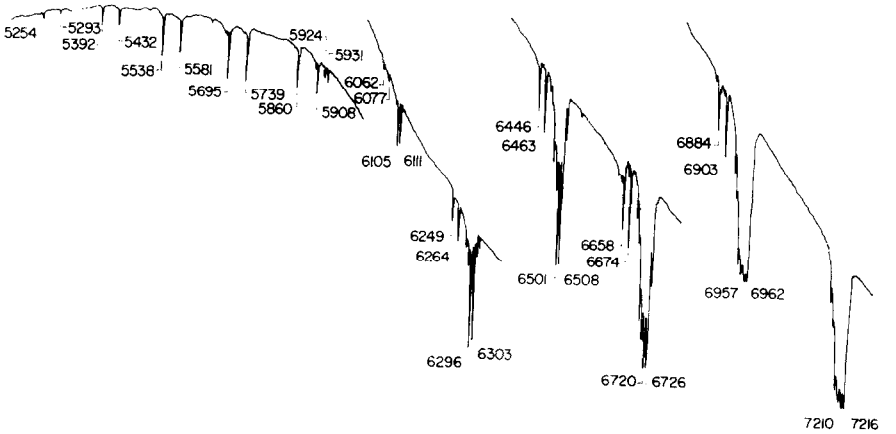

FIG. 4. Absorption spectrum of the A system of BS_2 for a sample containing equal amounts of ^{10}B and ^{11}B isotopes. Wavelengths are in Å.

TABLE II

ABSORPTION BANDS OF $^{10}BS_2$ A SYSTEM IN NEON AT 4°K

λ, Å[a]	Intensities[b]	λ, Å[a]	Intensities[b]
7210.0	0.93	6104.8	0.10
6956.8	1.00	6062.3	0.04
6883.9	0.16	6007.0	0.00
6766.8	0.01	5923.5	0.03
6719.8	0.91	5859.7	0.09
6657.9	0.21	5756.3	0.01
6580.5	0.01	5694.0	0.12
6549.3	0.01	5652.7	0.01
6501.5	0.80	5537.9	0.09
6446.4	0.15	5502.5	0.02
6376.8	0.01	5391.7	0.05
6344.5	0.01	5360.2	0.01
6296.0	0.36	5253.5	0.02
6248.5	0.08	5224.7	0.01
6185.8	0.01	5121.5	0.00
6153.5	0.00	5098.5	0.00

[a] Band positions are for sub-band *b* due to BS_2 in the predominant trapping site.

[b] The relative intensities observed were similar to the $^{11}BS_2$ bands and are listed as such.

A system. Figure 2 shows a spectrum of the A system obtained from vaporizing a ZnS-^{11}B sample into a neon matrix at 4°K. The shape of each band in the system is very similar and consists of a group of four or five sharp peaks. These sub-bands are attributed to multiple trapping sites of the BS_2 molecule in the solid neon matrix. An expanded view of the site splitting of the 6462.8 and 6507.8 Å bands is shown in Fig. 3. Absorption peaks due to sites labeled *a* to *d* were observed for medium to strong intensity bands. An additional sub-band *e* was observed for very strong intensity bands.

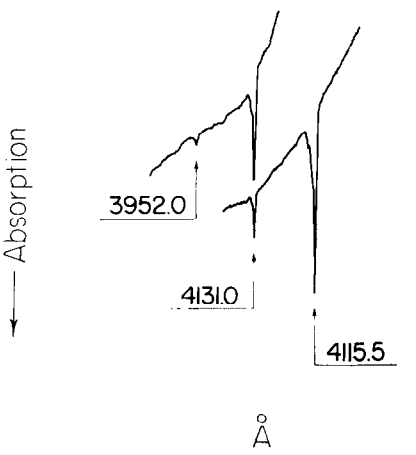

FIG. 5. Absorption spectrum of the B system of BS_2 isolated in Ne at 4°K.

TABLE III

ABSORPTION BANDS OF BS_2 B SYSTEM IN NEON AT 4°K

λ, Å	ν, cm^{-1}	$(v_1', 0^0, 0)^b$	ΔG, cm^{-1}
4115.5	24,292	(0, 0⁰, 0)	
			509[c]
4031.0	24,801	(1, 0⁰, 0)	
			495
3952.0	25,296	(2, 0⁰, 0)	

[a] Isotope shifts between $^{10}BS_2$–$^{11}BS_2$ were not measured.

[b] See analysis in text for explanation.

[c] 505 cm^{-1} in gas phase spectra of (5).

The weaker bands in the system showed only the peak due to the predominant trapping site *b*. The bandwidths observed were 4–8 cm^{-1} and allowed peak positions to be measured within ±0.5 Å (or 1–2 cm^{-1}). Progressions formed from the various sub-bands belonging to the different sites all gave uniform term separations. As such, we shall only refer to the predominant site sub-band in further analysis. Table I lists the absorption bands observed for $^{11}BS_2$ trapped in site *b*.

Similar spectra were obtained using ZnS-^{10}B samples, and the appearances of the bands due to multiple trapping sites of $^{10}BS_2$ in neon were the same as for $^{11}BS_2$. Figure 4 shows the spectrum observed when a boron sample containing approximately equal proportions of ^{10}B and ^{11}B was used. The important result here is that the absorption bands are grouped into doublets. This is the expected isotope effect for a transition belonging to a molecule containing a single B atom, namely $^{10}BS_2$ and $^{11}BS_2$. The positions of the bands for $^{10}BS_2$ in the predominant site in neon at 4°K are listed in Table II.

B system. The spectrum of BS_2 observed in the 4100 Å region is shown in Fig. 5. At higher resolution the shape of the bands indicate the presence of multiple site effects, although not as pronounced as for the A system bands. Isotope shifts between the $^{10}BS_2$ and $^{11}BS_2$ bands were not determined due to their small magnitude and to uncertainties from site splittings. An estimated upper limit for the ^{10}B-^{11}B shift in the 4116 Å band is 6 cm^{-1}. Table III lists the observed band positions.

Unidentified Bands. Analysis of the visible spectra, as given below, has shown that all but a few of the large number of bands observed throughout the region 3500–12,000 Å can be assigned to the two systems of BS_2. Occasionally, weak bands were measured at 4750, 4563, 4400, 4367, 4354, 4045, and 4021 Å that remain unidentified. Although BS_2 is the predominant molecule in the matrix, the IR spectra reveal that several additional molecules are present so that added absorption bands are not unexpected. The concentration of Zn atoms in the matrix ought to be high (*4*); however, the spectrum expected for Zn lies in the ultraviolet (*9*).

II. Analysis of Visible Spectra

The analysis of the visible spectrum of BS_2 parallels that of the gas phase spectrum of BO_2 (*1*). Supported by the analysis presented here, we may assume that the electronic

configurations giving rise to the ground and excited states of BS_2 are the same as those for BO_2:

$$\cdots \quad (\sigma_g)^2(\sigma_u)^2(\sigma_g)^2(\sigma_u)^2(\pi_u)^4(\pi_g)^3,\ X^2\Pi_{g(\text{inverted})},$$

$$\cdots \quad \cdots \quad \cdots \quad (\sigma_g)^2(\sigma_u)^2(\pi_u)^3(\pi_g)^4,\ A^2\Pi_{u(\text{inverted})},$$

and

$$\cdots \quad \cdots \quad \cdots \quad (\sigma_g)^2(\sigma_u)^1(\pi_u)^4(\pi_g)^4,\ B^2\Sigma_u^+.$$

The 7200 Å and 4100 Å systems of BS_2 are then assigned to $A^2\Pi_u$–$X^2\Pi_g$ and $B^2\Sigma_u^+$–$X^2\Pi_g$ transitions, respectively.

At 4°K each band is considered to arise in transition from the zero-point $^2\Pi_{g,\frac{1}{2}}$ vibronic level of the ground state. The bands are identified by (v_1', $v_2'^l$, v_3') which designates the particular $^2\Pi_{u,\frac{3}{2}}$ or $^2\Sigma_u^+$ vibronic levels of the $A^2\Pi_u$ or $B^2\Sigma_u^+$ excited states, respectively, where l is the angular momentum quantum number associated with the bending vibration of a linear triatomic molecule. By the Franck–Condon principle for linear-linear transitions, the v_1' progressions involving the symmetric stretching vibration are strongly allowed, whereas progressions of the $2v_2'$ bending and $2v_3'$ antisymmetric stretching vibrations are expected to be weak.

A system. The strongest bands in the A system form the (v_1', 0^0, 0) progression, as expected, and the isotopic data support this assignment. Table IV lists the (v_1', 0^0, 0) bands and gives the resulting vibrational constants for $^{10}BS_2$ and $^{11}BS_2$. There is no isotope shift predicted for the symmetric stretching frequencies, and the $\omega_1^{0'}$ values are observed to be the same for both molecules.

TABLE IV

(v_1', 0^0, 0) PROGRESSIONS OF $^{10}BS_2$ AND $^{11}BS_2$

$^{10}BS_2$				$^{11}BS_2$			
λ, Å	ν, cm^{-1}	(v_1', 0^0, 0)	ΔG, cm^{-1}	λ, Å	ν, cm^{-1}	(v_1', 0^0, 0)	ΔG, cm^{-1}
7210.0	13,866	(0, 0^0, 0)		7216.0	13,854	(0, 0^0, 0)	
			505				505
6956.8	14,371	(1, 0^0, 0)		6962.5	14,359	(1, 0^0, 0)	
			506				505
6719.8	14,877	(2, 0^0, 0)		6725.8	14,864	(2, 0^0, 0)	
			500				498
6501.5	15,377	(3, 0^0, 0)		6507.8	15,362	(3, 0^0, 0)	
			501				499
6296.0	15,878	(4, 0^0, 0)		6302.8	15,861	(4, 0^0, 0)	
			498				498
6104.8	16,376	(5, 0^0, 0)		6111.2	16,359	(5, 0^0, 0)	
			501				497
5923.6	16,877	(6, 0^0, 0)		5931.0	16,856	(6, 0^0, 0)	
			490				489
5756.3	17,367	(7, 0^0, 0)		5763.8	17,345	(7, 0^0, 0)	
	$\omega_1^{0'} = 506(1)$ cm^{-1}				$\omega_1^{0'} = 506(1)$ cm^{-1}		
	$X_{11}^{0'} = -1(1)$ cm^{-1}				$X_{11}^{0'} = -1(1)$ cm^{-1}		

TABLE V

(v_1', 2^0, 0) AND (v_1', 0^0, 2) PROGRESSIONS OF $^{10}BS_2$ AND $^{11}BS_2$

$^{10}BS_2$				$^{11}BS_2$			
λ, Å	ν, cm^{-1}	(v_1', 2^0, 0)	ΔG, cm^{-1}	λ, Å	ν, cm^{-1}	(v_1', 2^0, 0)	ΔG, cm^{-1}
6883.9	14,523	(0, 2^0, 0)		6903.0	14,482	(0, 2^0, 0)	
			493				496
6657.9	15,016	(1, 2^0, 0)		6674.0	14,978	(1, 2^0, 0)	
			492				492
6446.4	15,508	(2, 2^0, 0)		6462.5	15,470	(2, 2^0, 0)	
			491				492
6248.5	15,999	(3, 2^0, 0)		6263.0	15,962	(3, 2^0, 0)	
			492				490
6062.3	16,491	(4, 2^0, 0)		6076.7	16,452	(4, 2^0, 0)	
		$X_{12}^{0'} = -6(1)$ cm^{-1}				$X_{12}^{0'} = -4(1)$ cm^{-1}	
5859.7	17,061	(0, 0^0, 2)		5907.3	16,924	(0, 0^0, 2)	
			496				496
5694.0	17,557	(1, 0^0, 2)		5739.0	17,420	(1, 0^0, 2)	
			495				495
5537.9	18,052	(2, 0^0, 2)		5580.4	17,915	(2, 0^0, 2)	
			490				489
5391.7	18,542	(3, 0^0, 2)		5432.0	18,404	(3, 0^0, 2)	
			488				485
5253.5	19,030	(4, 0^0, 2)		5292.5	18,889	(4, 0^0, 2)	
			490				482
5121.5	19,520	(5, 0^0, 2)		5161.0	19,371	(5, 0^0, 2)	
		$X_{13}^{0'} = -6(1)$ cm^{-1}				$X_{13}^{0'} = -5(1)$ cm^{-1}	

For the two nontotally symmetric vibrations, ν_2 and ν_3, the ratio of the isotopic frequencies of $^{10}BS_2$ to $^{11}BS_2$ is calculated to be 1.04158 in the harmonic approximation and in the absence of Fermi resonance effects. The bands at 6883.9 and 6903.3 Å are then assigned to the (0, 2^0, 0) transition of $^{10}BS_2$ and $^{11}BS_2$, respectively, because the resulting $2\nu_2'$ values of 655(2) cm^{-1} ($^{10}BS_2$) and 629(2) cm^{-1} ($^{11}BS_2$), as averaged from all the sub-bands, give an observed isotopic ratio of 1.041(3) and are the right order of magnitude to be expected for bending frequencies. The (0, 2^0, 0) bands are also the origin of another progression, namely (v_1', 2^0, 0), as listed in Table V. Similar considerations apply to the weak bands at 5859.7 and 5907.3 Å, that are assigned to the (0, 0^0, 2) transition of $^{10}BS_2$ and $^{11}BS_2$, respectively. The average $2\nu_3'$ values are then 3192(3) cm^{-1} ($^{10}BS_2$) and 3069(2) cm^{-1} ($^{11}BS_2$) with an observed isotopic ratio of 1.0401(9). The (0, 0^0, 2) bands also serve as the origin of the (v_1', 0^0, 2) progressions which are included in Table V.

Very weak bands are observed at 5652.7 and 5704.5 Å which are 625 and 601 cm^{-1} above the (0, 0^0, 2) bands af $^{10}BS_2$ and $^{11}BS_2$, respectively. These are assigned as the (0, 2^0, 2) transitions, and they are the origins for another progression in v_1', the (v_1', 2^0, 2) progression which is listed in Table VI. Similarly, weak bands at 6580.5 and 6609.3 Å

TABLE VI

(v_1', 2^0, 2) PROGRESSIONS OF $^{10}BS_2$ AND $^{11}BS_2$

$^{10}BS_2$				$^{11}BS_2$			
λ, Å	ν, cm^{-1}	(v_1', 2^0, 2)	ΔG, cm^{-1}	λ, Å	ν, cm^{-1}	(v_1', 2^0, 2)	ΔG, cm^{-1}
5652.7	17,686	(0, 2^0, 2)		5704.5	17,525	(0, 2^0, 2)	
			483				483
5502.5	18,169	(1, 2^0, 2)		5551.7	18,008	(1, 2^0, 2)	
			482				481
5360.2	18,651	(2, 2^0, 2)		5407.0	18,489	(2, 2^0, 2)	
			484				483
5224.7	19,135	(3, 2^0, 2)		5269.5	18,972	(3, 2^0, 2)	
			473				478
5098.5	19,608	(4, 2^0, 2)		5140.0	19,450	(4, 2^0, 2)	

are 669 and 644 cm^{-1} above the (0, 2^0, 0) bands of $^{10}BS_2$ and $^{11}BS_2$. respectively, The intensities and wavenumber shifts suggest that these are the (0, 4^0, 0) bands. Weak intensity progressions are also observed and assigned to (v_1', 4^0, 0) bands, as listed in Table VII.

As observed, the (0, 2^0, 0) and (0, 4^0, 0) bands imply that the $\omega_2^{0'}$ values are 324(2) and 311(2) cm^{-1}, with $X_{22}^{0'}$ anharmonicity constants of $+2(1)$ cm^{-1}, for $^{10}BS_2$ and $^{11}BS_2$, respectively. These results give an isotopic ratio of 1.040(3) compared to the calculated value of 1.04158.

A large number of bands in system A have been assigned without necessary consideration of spin-orbit or vibronic (Renner–Teller) interactions. In the absence of any Renner–Teller effect the spin-orbit effects should not be observed since it is presumed that all BS_2 molecules are present in the $^2\Pi_{\frac{1}{2}}$ level of the ground state at 4°K and the selection rule $\Delta\Sigma = 0$ holds for Hund's case *a* coupling (*10*). With vibronic interaction the selection rule $\Delta P = 0$, where $P = |\Lambda + l + \Sigma|$, allows a transition from the (0, 0^0, 0)

TABLE VII

(v_1', 4^0, 0) PROGRESSIONS OF $^{10}BS_2$ AND $^{11}BS_2$

$^{10}BS_2$				$^{11}BS_2$			
λ, Å	ν, cm^{-1}	(v_1', 4^0, 0)	ΔG, cm^{-1}	λ, Å	ν, cm^{-1}	(v_1', 4^0, 0)	ΔG, cm^{-1}
6580.5	15,192	(0, 4^0, 0)		6609.3	15,126	(0, 4^0, 0)	
			486				484
6376.8	15,678	(1, 4^0, 0)		6404.5	15,610	(1, 4^0, 0)	
			484				485
6185.8	16,162	(2, 4^0, 0)		6211.5	16,095	(2, 4^0, 0)	
			481				486
6007.0	16,643	(3, 4^0, 0)		6029.3	16,581	(3, 4^0, 0)	

TABLE VIII

(v_1', 2^2, 0) PROGRESSIONS OF $^{10}BS_2$ AND $^{11}BS_2$

$^{10}BS_2$				$^{11}BS_2$			
λ, Å	ν, cm^{-1}	(v_1', 2^2, 0)	ΔG, cm^{-1}	λ, Å	ν, cm^{-1}	(v_1', 2^2, 0)	ΔG, cm^{-1}
6766.8	14,774	(0, 2^2, 0)		6784.3	14,736	(0, 2^2, 0)	
			491				491
6549.3	15,265	(1, 2^2, 0)		6565.5	15,227	(1, 2^2, 0)	
			492				489
6344.5	15,757	(2, 2^2, 0)		6361.3	15,716	(2, 2^2, 0)	
			489				491
6153.5	16,246	(3, 2^2, 0)		6168.5	16,207	(3, 2^2, 0)	

$^2\Pi_{\frac{3}{2}}$ vibronic level of the ground state to the (0, 2^2, 0) $^2\Pi_{\frac{3}{2}}$ vibronic level of the $A^2\Pi_{\frac{1}{2}}$ excited state (*1*). Again, the transition intensity is predicted to be weak by the Franck–Condon principle. The weak bands at 6766.8 and 6784.3 Å in the $^{10}BS_2$ and $^{11}BS_2$ spectra, respectively, are assigned as the (0, 2^2, 0) bands and a progression of (v_1', 2^2, 0) bands is also observed as listed in Table VIII. The splitting of the (0, 2^0, 0) and (0, 2^2, 0) bands is due to the combined effects of spin–orbit and vibronic interactions (*11*). However, the vibronic interaction parameter, $\epsilon\omega^{2'}$, in the excited state is likely to be small (*1*) compared to the bending frequency and the spin–orbit constant. Then the (0, 2, 0) band splitting gives an approximate value for the spin–orbit splitting of the $A^2\Pi_u$ state of -253 cm^{-1}. The observation of weak bands due to vibronic interactions gives support to the assignment of the excited state of the A system as a degenerate electronic state. Support for this value of the spin–orbit constant of the $A^2\Pi_u$ state is also derived from the analysis of a very weak system assigned to the $A^2\Pi_{\frac{1}{2}}$–$X^2\Pi_{\frac{3}{2}}$ transition, as presented below.

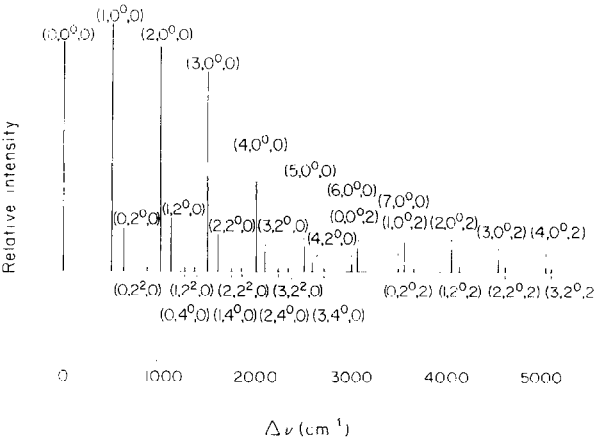

FIG. 6. Schematic of the $A^2\Pi_u$–$X^2\Pi_g$ spectrum of BS_2.

A schematic of the overall spectrum of the A system is shown in Fig. 6. All of the progressions in ν_1' are remarkably regular and are consistent with the derived vibrational constants. In each progression the band having $\nu_1' = 1$ is the most intense indicating a substantial change in the B-S bond length between the two states.

B system. Only three bands are observed in the *B* system spectrum of BS_2. The bands fit a progression and the absence of an isotope shift along with the similarity of the term separations with the symmetric stretching frequency of the $A^2\Pi_u$ state allows them to be assigned as the (v_1', 0^0, 0) progression, as listed in Table III. The vibrational constants obtained for the $B^2\Sigma_u^+$ state are then $\omega_1^{0'} = 516$ cm^{-1} and $X_{11}^{0'} = -7$ cm^{-1}. This assignment is in agreement with $\nu_1' = 505$ cm^{-1} given by Koryazhkin and Mal'tsev (5) from gas phase spectra (see Discussion).

$A^2\Pi_{\frac{1}{2}}$–$X^2\Pi_{\frac{3}{2}}$ *system.* As mentioned above, the $A^2\Pi_{u,\frac{1}{2}}$–$X^2\Pi_{g,\frac{3}{2}}$ transition is not allowed in case *a* coupling due to the selection rule $\Delta\Sigma = 0$. However, for large values of the spin–orbit constant in one of the II states the coupling may approach case *c*, and then the $^2\Pi_{\frac{1}{2}}$–$^2\Pi_{\frac{3}{2}}$ transition becomes weakly allowed (*10*). Very weak intensity bands are observed at 7076 and 6831 Å in the $^{10}BS_2$ spectrum, and at 7081 and 6837 Å in the $^{11}BS_2$ spectrum which may be discerned in Fig. 2. The 7076 and 7081 Å bands are assigned to the (0, 0^0, 0) $^2\Pi_{\frac{1}{2}}$ transitions giving a spin–orbit constant of $-263(2)$ cm^{-1} for the $A^2\Pi_u$ state. The 6831 and 6837 Å bands are then the (1, 0^0, 0) $^2\Pi_{\frac{1}{2}}$ bands at 507(2) and 504(2) cm^{-1} above the (0, 0^0, 0) $^2\Pi_{\frac{1}{2}}$ bands of $^{10}BS_2$ and $^{11}BS_2$, respectively.

The true spin–orbit constant determined here is close to the value, -253 cm^{-1}, estimated from the separation of the (0, 2^0, 0) $^2\Pi_{\frac{3}{2}}$ and (0, 2^2, 0) $^2\Pi_{\frac{3}{2}}$ bands. It would be expected that the splitting of the (0, 2^l, 0) bands would be larger in absolute value than the spin–orbit splitting if vibronic effects occur (*11*), as in BO_2. This may be seen from

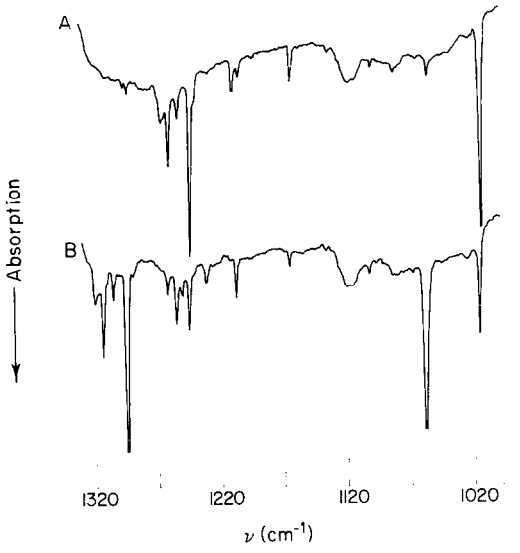

FIG. 7. Infrared absorption spectra of B-S samples isolated in Ne at 4°K: A, samples containing predominantly ^{11}B isotope; B, samples containing predominantly ^{10}B isotope.

TABLE IX

OBSERVED ISOTOPE PAIRS OF INFRARED BANDS FOR NEON MATRICES AT 4°K

^{10}B ν, cm^{-1}	Assignment	^{11}B ν, cm^{-1}
1056.7	ν_3 BS_2	1014.6
1207.3	ν BS	1165.3
1254.8	ν_3 B_2S_2	1211.2
1294.0	ν_1 B_2S_2 (?)	1244.5
1312.4	ν_6 B_2S_2 (?)	1261.3

Eq. 1 of Johns (*1*) which shows that any value of the Renner parameter, $\epsilon\omega_2'$, will increase the effective A′ value, since states with the same P quantum number repel each other. The fact that the splitting is smaller in absolute magnitude than -263 cm^{-1} indicates only a small degree of vibronic coupling in the $A^2\Pi_u$ state. Fermi resonance effects (*12*) might explain the smaller value since in BO_2 $\nu_1' > 2\nu_2'$, whereas here $\nu_1' < 2\nu_2'$ and the resonance would shift the (0, 2^0, 0) level closer to the (0, 2^2, 0). However, the splittings of all the (ν_1', 2^l, 0) $^2\Pi_{\frac{3}{2}}$ bands are very regular, and indeed the lack of irregularities in each of the observed progressions would seem to indicate that Fermi resonance effects in the $A^2\Pi_u$ state are quite small. The change in the spin–orbit splitting may then reflect a small variation of the A′ value with the bending vibrational quantum number, although the exact way that A′ should vary with ν_2' is not known (*11*). Of course, the other indications demonstrate that vibronic interaction is present, but it must be hidden here by these other small effects. Note that the intensity of the (0, 2^2, 0) $^2\Pi_{\frac{3}{2}}$ band is larger than that of the (0, 0^0, 0) $^2\Pi_{\frac{3}{2}}$ or (1, 0^0, 0) $^2\Pi_{\frac{3}{2}}$ bands indicating that the transition allowed by vibronic interaction is stronger than that allowed by the approach to case c coupling.

III. Infrared Absorption Spectra

Numerous absorption bands were observed in the 1000–1325 cm^{-1} region of the IR spectrum. Spectra obtained when samples containing predominantly the ^{11}B or ^{10}B isotope were used indicated several isotopic pairs of bands, as shown in Fig. 7 and listed in Table IX. The spectrum of a sample containing approximately equal amounts of ^{10}B and ^{11}B, shown in Fig. 8, was interesting since it indicated that the isotopic spectra were almost additive. No *strong* bands due to a mixed ^{10}B-^{11}B species were observed.

BS_2 spectrum. The very strong bands at 1014.6 and 1056.7 cm^{-1} are assigned to the asymmetric stretching frequency, ν_3, of $^{11}BS_2$ and $^{10}BS_2$, respectively. Although the absolute frequencies are measured to ± 0.5 cm^{-1}, the relative frequencies have an uncertainty of ± 0.2 cm^{-1}. The observed frequency ratio for the isotopic bands is 1.0415(5) and is in reasonable agreement with the Teller–Redlich ratio of 1.04158 calculated for linear symmetric BS_2. The symmetric stretching band of linear BS_2 is forbidden in the IR, and the bending vibration is estimated to lie below the 200 cm^{-1} limit of the spectrometer (see Discussion).

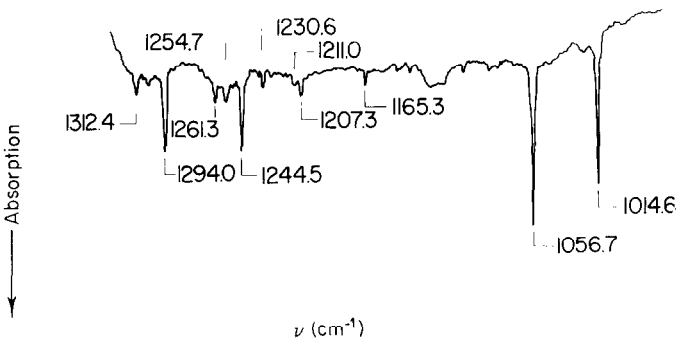

FIG. 8. Infrared absorption spectrum of B-S sample containing equal amounts of ^{10}B and ^{11}B isotopes.

The ν_3 frequency measured here may be compared to a tentative value of 910 cm^{-1} assigned to BS_2 by Greene (*13*). Sommer, Walsh, and White (*4*) observed bands at 993 and 1052 cm^{-1} in IR emission from the gas phase over heated ^{11}B-ZnS and ^{10}B-ZnS samples, respectively. The bands were assigned to a B-S stretching frequency although it was uncertain whether they belonged to BS_2 or to B_2S_3. Their bands are fairly close to the 1014.6 and 1056.7 cm^{-1} bands observed here for BS_2.

BS and B_2S_2 spectrum. Weak bands observed at 1165.3 and 1207.3 cm^{-1} are assigned to ^{11}BS and ^{10}BS, respectively (*14, 15*). Similarly, weak bands observed at 1211.2 and 1254.8 cm^{-1} are assigned to the asymmetric stretching frequency of linear symmetric $^{11}B_2S_2$ and $^{10}B_2S_2$, respectively. The observed frequency ratio is 1.0360(5) which is close to the value calculated by the Teller–Redlich rule of 1.03635. The band due to the mixed species $^{10}B^{11}BS_2$ is observed at 1230.6 cm^{-1} (this was the only band which was assignable to a ^{10}B-^{11}B species in the spectrum shown in Fig. 8). These B_2S_2 data are in agreement with the gas phase results of Sommer, Walsh, and White (*4*).

B_2S_3(?) spectrum. In the 1250 and 1300 cm^{-1} regions several bands of strong to medium intensity were observed for ^{11}B and ^{10}B samples, respectively. The ^{10}B group consists of bands at 1294.0, 1304.2, 1312.4, and 1318.4 cm^{-1} while a similar group for ^{11}B samples appears at 1244.5, 1254.8 (overlapped with $^{10}B_2S_2$ band), 1261.3, and 1266.5 cm^{-1}. These bands are in the region where vibrations of B_2S_3 would be expected to appear (*3, 4, 13*), and the bands at 1294.0 and 1312.4 cm^{-1} and at 1244.5 and 1261.3 cm^{-1} can be assigned to ν_1 (B = S sym. str.) and ν_6 (B = S asym. str.) of $^{10}B_2S_3$ and $^{11}B_2S_3$, respectively, by analogy with B_2O_3 studies (*8, 16*). However, there are difficulties with this assignment since the mixed isotope spectrum shows no strong bands due to $^{10}B^{11}BS_3$; however, a similar situation did occur in the IR study of B_2O_3. Also, there should be several additional bands due to B_2S_3 in other regions of the IR spectrum which are not observed. These assignments must then be considered tentative until additional data can clarify the situation.

IV. Visible Emission Spectrum

Attempts to observe the optical emission spectra in the usual manner were not performed in this series of experiments. However, a weak emission band, shown in Fig. 9,

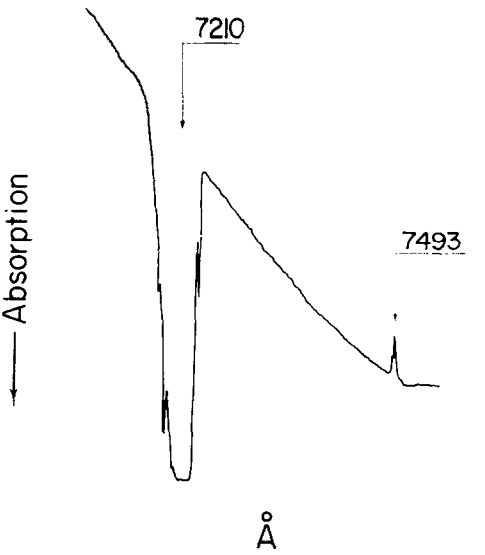

FIG. 9. Spectrum of BS_2 in Ne at 4°K showing 7493 Å band observed in emission along with intense 7210 Å band observed in absorption.

was consistently observed at 7493 Å during the recording of the absorption spectra. The 510 cm^{-1} separation to longer wavelengths suggests that the emission is due to the transition from the (0, 0^0, 0) level of the $A^2\Pi_u$ state to the (1, 0^0, 0) level of the ground state. If this is correct then the symmetric stretching frequency for each of the three observed states of BS_2 is about the same, a result similar to that found for BO_2 (*1*).

DISCUSSION

The analysis of the BS_2 spectrum presented here differs from the conclusions given by Koryazhkin and Mal'tsev (KM) (*5*). These authors observed the electronic spectrum of the vapors over B_2S_3(s), B(s) + S(s), or B_2O_3(s) + Al_2S_3(s) samples heated to 900–1200°C. Similarly, they recorded bands in the 8000–6100 Å and 4100 Å regions which they assigned to $A^2\Pi_u$–$X^2\Pi_g$ and $B^2\Sigma_u^+$–$X^2\Pi_g$ transitions of BS_2, respectively. Their B system bands at 4095 and 4012 Å agree well with our matrix results, and they have assigned them similarly. They also observed a band at 4171 Å which they assigned to a (0, 0^0, 0)–(1, 0^0, 0) transition. However, the 4171 Å band is 440 cm^{-1} to the red of the 4095 Å (0, 0^0, 0) $^2\Sigma^+$–(0, 0^0, 2) $^2\Pi_{\frac{1}{2}}$ band, and it is more likely that the former is a (0, 0^0, 0) $B^2\Sigma^+$–(0, 0^0, 0) $X^2\Pi_{\frac{1}{2}}$ hot band. If this is correct then the spin-orbit splitting in the $X^2\Pi_g$ state of BS_2 would be -440 cm^{-1}, a value which is in agreement with that for CS_2^+ in its ground state, as determined by Callomon (*17*). This is in accord with the similar findings of Johns (*1*, *18*) when comparing the isoelectronic BO_2 and CO_2^+ molecules. The π_g molecular orbital of BS_2 is essentially pure S($3p\pi$) since it is nonbonding, and Callomon (*17*) has shown that the spin–orbit splitting of -440 cm^{-1} in the $X^2\Pi_g$ state of CS_2^+ is consistent with this fact. Excitation to a bonding π_u orbital, involving both B($2p\pi$) and S($3p\pi$), as occurs in the $A^2\Pi_u$ state of BS_2,

TABLE X

COMPARISON OF GAS PHASE AND NEON MATRIX SPECTRA OF $^{11}BS_2$

Transition	Matrix,[a] Å	ΔG, cm^{-1}	Gas,[b] Å	ΔG, cm^{-1}
(0, 0⁰, 0)	7216.0		6923.7	
		505		496
(1, 0⁰, 0)	6962.5		6693.7	
		505		492
(2, 0⁰, 0)	6725.8		6481.2	
		498		473
(3, 0⁰, 0)	6507.8		6287	
		499		490
(4, 0⁰, 0)	6302.8		~6100	

[a] Data here are same as those in Table IV.

[b] Reinterpretation of data presented by Koryazhkin and Mal'tsev (5).

should lead to a decrease in spin–orbit splitting because of the smaller constant for boron and our measured value of -263 cm^{-1} reflects this.

Furthermore, KM have interpreted their A system spectrum to present evidence that BS_2 is bent in either the $A^2\Pi_u$ or $X^2\Pi_g$ state, but their analysis of the A system contains several inconsistencies. A reinterpretation of their data can reasonably be given which brings their results into much closer agreement with ours. Such a reinterpretation is presented in Table X along with a comparison with the matrix data. Their intense 6923.7 Å band is there reassigned as the (0, 0⁰, 0) $^2\Pi_{\frac{3}{2}}$ band to obtain a (v_1', 0⁰, 0) progression consistent with ours. We would then assign their 7004.2 Å band as a hot band due to the (0, 0⁰, 0) $A^2\Pi_{\frac{1}{2}}$–(0, 0⁰, 0) $X^2\Pi_{\frac{1}{2}}$ transition; the shoulders observed on their (v_1', 0, 0⁰) $^2\Pi_{\frac{3}{2}}$ progression then belong to the (v_1', 0⁰, 0) $^2\Pi_{\frac{3}{2}}$ progression. (Other hot bands involving the bending frequency of the $X^2\Pi_g$ state are also likely in their spectra and probably contribute to the width of their bands.) The above interpretation of their data implies that the difference in the spin–orbit splitting of the two Π states is ~166 cm^{-1} compared to our estimate of ~177 cm^{-1}. The ill-defined bands in the 7200–8000 Å

TABLE XI

VIBRATIONAL FREQUENCIES AND FORCE CONSTANTS OF $^{11}BS_2$

	$X^2\Pi_g$	$A^2\Pi_u$
ν_1 (Σ_g^+)[a]	510	506
ν_2 (Π_u)	~120	311
ν_3 (Σ_u^+)	1015	1535
f_r[b]	3.9	5.7
f_{rr}	1.0	−0.9
f_α/r^2	0.02	0.14

[a] Frequencies are in cm^{-1}.

[b] Force constants are in mdyn/Å.

region of their spectrum are probably due to other species in the vapor over their samples.

All of the vibrational frequencies in the $A^2\Pi_u$ state, and all but the bending frequency in the $X^2\Pi_g$ state have been measured directly from the observed spectra; Table XI lists the results. A reliable estimate of the bending frequency in the ground state is available from the isotope shift in the (0, 0^0, 0) band of system *A*. Assuming that $\nu_2(^{10}BS_2)/\nu_2(^{11}BS_2) = 1.0416$, the data gives $\nu_2(^{11}BS_2) \simeq 120$ cm^{-1}. A larger value for the bending frequency in the $A^2\Pi_u$ state is consistent with the stabilizing influence that the number of π_g electrons has on the linear conformation of the molecule, as discussed by Herzberg (*2*).

Force constants have been calculated from the observed frequencies in the two lowest states of BS_2 and are included in Table XI. The magnitude of f_r allows an estimate to be made for the B-S bond distance in the molecule, for both electronic states, by using the appropriate Laurie–Herschbach relation (*19*)

$$r = 2.02 - 0.53 \log f_r.$$

The values obtained for r(B-S) are 1.7 and 1.6 Å in the $X^2\Pi_g$ and $A^2\Pi_u$ states, respectively. (Similar calculations using the BO_2 data (*1*) give r(B-O) distances within 0.1 Å of the observed values.) The BS_2 bond distances are consistent with the signs and magnitudes of the f_{rr} interaction constants calculated in the two different electronic states. If the dissociation products of BS_2 are given by

$$\begin{array}{lll} BS_2(X^2\Pi_g) \rightarrow BS(X^2\Sigma) + & S(^3P) & \\ r = 1.7 \qquad r = 1.6 & \Delta r = +0.1, & \end{array}$$

and

$$\begin{array}{lll} BS_2(A^2\Pi_u) \rightarrow BS(A^2\Pi_i) + & S(^3P) & \\ r = 1.6 \qquad r = 1.8 & \Delta r = -0.2, & \end{array}$$

then the correlation (*20*) between the sign of the f_{rr} constant and the change in bond length as the triatomic molecule dissociates to the diatomic does predict a rather large positive and negative interaction constant in the $X^2\Pi_g$ and $A^2\Pi_u$ state, respectively, as observed

RECEIVED: July 24, 1972

ACKNOWLEDGMENTS

The authors gratefully acknowledge the support of the Air Force Office of Scientific Research under Grant AFOSR 72-2208.

REFERENCES

1. J. W. C. JOHNS, *Canad. J. Phys.* **39**, 1738 (1961).
2. G. HERZBERG, "Electronic Spectra of Polyatomic Molecules," p. 499. D. Van Nostrand, Princeton, 1966.
3. F. T. GREENE AND J. L. MARGRAVE, *J. Amer. Chem. Soc.* **81**, 5555 (1959).
4. A. SOMMER, P. N. WALSH, AND D. WHITE, *J. Chem. Phys.* **33**, 296 (1960).
5. V. A. KORYAZHKIN AND A. A. MAL'TSEV, *Vestn. Mosk. Univ., Ser. 2, Khim.* **21**, 6 (1966).

6. F. T. GREENE AND P. W. GILLES, *J. Amer. Chem. Soc.* **84**, 3598 (1962); F. T. GREENE AND P. W. GILLES, *J. Amer. Chem. Soc.* **86**, 3964 (1964); H. CHEN AND P. W. GILLES, *J. Amer. Chem. Soc.* **92**, 2309 (1970).
7. YA. KH. GRINBERG, E. G. ZHUKOV, AND V. A. KORYAZHKIN, *Dokl. Akad. Nauk SSSR* **190**, 589 (1970).
8. W. WELTNER, JR. AND J. R. W. WARN, *J. Chem. Phys.* **37**, 292 (1962); W. WELTNER, JR., P. N. WALSH, AND C. L. ANGELL, *J. Chem. Phys.* **40**, 1299 (1964); W. WELTNER, JR. AND D. MCLEOD, JR., *J. Chem. Phys.* **40**, 1305 (1964).
9. W. W. DULEY, *Nature* **210**, 624 (1966).
10. G. HERZBERG, "Spectra of Diatomic Molecules." D. Van Nostrand, New York, 1950.
11. J. A. POPLE, *Mol. Phys.* **3**, 16 (1960); J. T. HOUGEN, *J. Chem. Phys.* **36**, 519 (1962).
12. J. T. HOUGEN, *J. Chem. Phys.* **37**, 403 (1962).
13. F. T. GREENE, *Diss. Abstr.* **22**, 1838 (1961).
14. P. B. ZEEMAN, *Can. J. Phys.* **29**, 336 (1951).
15. J. M. BROM, JR. AND W. WELTNER, JR., *J. Chem. Phys.*, submitted for publication.
16. A. SOMMER, D. WHITE, M. J. LINEVSKY, AND D. E. MANN, *J. Chem. Phys.* **38**, 87 (1963).
17. J. H. CALLOMON, *Proc. Roy. Soc. Ser. A* **244**, 220 (1958).
18. J. W. C. JOHNS, *Canad. J. Phys.* **42**, 1004 (1964).
19. D. H. HERSCHBACH AND V. W. LAURIE, *J. Chem. Phys.* **35**, 458 (1961).
20. K. MACHIDA AND J. OVEREND, *J. Chem. Phys.* **50**, 4437 (1969).